BASIC SCIENCE RESEARCH ARTICLE

MUSCLE&NERVE WILEY

Regenerative peripheral nerve interface free muscle graft mass and function

Yaxi Hu MD[1,2] | Daniel C. Ursu PhD[1] | Racquel A. Sohasky BS[1] | Ian C. Sando MD[1] | Shoshana L. W. Ambani MD[1] | Zachary P. French MD[1] | Elizabeth A. Mays PhD[1] | Andrej Nedic MD[1] | Jana D. Moon BS[1] | Theodore A. Kung MD[1] | Paul S. Cederna MD[1,3] | Stephen W. P. Kemp PhD[1,3] [ID] | Melanie G. Urbanchek PhD[1]

[1]Department of Surgery, Section of Plastic and Reconstructive Surgery, University of Michigan, Ann Arbor, Michigan

[2]Department of Plastic Surgery, University of Groningen, Groningen, The Netherlands

[3]Department of Biomedical Engineering, University of Michigan, Ann Arbor, Michigan

Correspondence

Stephen W. P. Kemp, Department of Biomedical Engineering, Section of Plastic Surgery, University of Michigan, 1150 W Medical Center Drive, MSRB II, A570, Ann Arbor, MI 48109-5456, USA.
Email: swpkemp@med.umich.edu

Abstract

Background: Regenerative peripheral nerve interfaces (RPNIs) transduce neural signals to provide high-fidelity control of neuroprosthetic devices. Traditionally, rat RPNIs are constructed with ~150 mg of free skeletal muscle grafts. It is unknown whether larger free muscle grafts allow RPNIs to transduce greater signal.

Methods: RPNIs were constructed by securing skeletal muscle grafts of various masses (150, 300, 600, or 1200 mg) to the divided peroneal nerve. In the control group, the peroneal nerve was transected without repair. Endpoint assessments were conducted 3 mo postoperatively.

Results: Compound muscle action potentials (CMAPs), maximum tetanic isometric force, and specific muscle force were significantly higher for both the 150 and 300 mg RPNI groups compared to the 600 and 1200 mg RPNIs. Larger RPNI muscle groups contained central areas lacking regenerated muscle fibers.

Conclusions: Electrical signaling and tissue viability are optimal in smaller as opposed to larger RPNI constructs in a rat model.

KEYWORDS
EMG, muscle graft, prosthesis control, regeneration, RPNI

1 | INTRODUCTION

Innovations in robotic technology have led to the development of myoelectric prostheses capable of imitating precise hand, wrist, and finger movements.[1-3] Although advanced prostheses offer biomimetic

replacement of lost function, a majority of patients reject these sophisticated devices, preferring to use less functional, although more practical, body-powered prostheses.[4] A major reason for prosthetic abandonment is the lack of an optimal interface between the patient and the myoelectric prosthesis control.[5] The peripheral nerve is the ideal anatomic site for signal transduction of multiple motor and sensory nerves with a high degree of selectivity.[6] However, using electrodes to interface directly with peripheral nerves causes iatrogenic nerve injury and scarring, which ultimately compromises signal fidelity and quality.[7-10] By contrast, intramuscular and epimysial electromyography (EMG) can transfer muscle-specific efferent information to a prosthetic device through amplification of neural signals. The advantages of epimysial and intramysial electrodes are they:

(a) have less impedance; (b) can be physically more robust; (c) produce no neural damage, and; (d) provide amplification of very small nerve signals thus providing more favorable signal-to-noise ratios (SNRs), which can be used to power prosthetic devices.[11] In terms of surface electrodes, repeated signal calibration and reduced specificity remain problems that limit the degrees of freedom available for volitional prosthetic control.[12]

The regenerative peripheral nerve interface (RPNI) was developed as a strategy to optimize neural interfacing by addressing problems of direct electrode-nerve contact with the inherent limited signaling capacity.[13-17] RPNIs are neuromuscular biological interfaces surgically constructed with free skeletal muscle grafts (traditionally $3 \times 1.5 \times 0.5$ cm) obtained from skeletal muscle within the residual limb or from a distant site.[18,19] Residual peripheral nerves are dissected into single nerve fascicles, or groups of fascicles, to create functional units. The denervated muscle grafts are then neurotized by the terminal branches of the residual nerves. Muscle graft revascularization, nerve regeneration, and eventual graft reinnervation allow the RPNI to mature within 3 mo following surgical construction.[17-19] Previous studies in our laboratory have shown that RPNIs transduce evoked muscle potentials for up to 18 mo,[13] prevent neuroma formation,[18] and amplify motor nerve signals in animal models.[17,20,21] Thus, RPNI technology takes advantage of the neural signals acquired and transduced via intramuscular EMG to electrical signals, therefore eliminating the need for decoding multi-nerve motor features via classification algorithms.[22]

The maximal amount of free muscle that can be revascularized and neurotized by a peripheral nerve fascicle has not yet been determined. To date, rat RPNI models have used small skeletal muscle grafts weighing ~150 mg. However, use of larger muscle grafts could potentially further amplify transduced neural signals by producing a greater sum of muscle action potentials and provide more favorable SNR for higher fidelity control of neuroprosthetic devices. The purpose of the present work is to assess whether using free skeletal muscle grafts larger than 150 mg for constructing RPNIs increases peripheral nerve signal transduction in a rat model.

2 | METHODS

2.1 | Animals

Experiments were performed on F344 strain adult male rats (Harlan Laboratories, Haslett, Michigan, USA) at 3 mo of age, weighing approximately 250-315 g each. All animal care, housing, anesthesia, analgesia, surgical procedures, and terminal assessments were approved by the University of Michigan Institutional Animal Care and Use Committee.

2.2 | Experimental design

Thirty rats were randomly assigned to one of five study groups (n = 6 rats per group). In four experimental groups, a single RPNI per animal was constructed using a donor F344 rat semimembranosus (SM) free muscle graft weighing 150 mg (Group 1: RPNI 150), 300 mg (Group 2: RPNI 300), 600 mg (Group 3: RPNI 600), or 1200 mg (Group 4: RPNI

1200) per group. Donor SM muscle grafts were isolated, harvested, and trimmed longitudinally, in the direction of the muscle fibers, so as to achieve the desired mass within each group. The tendinous ends were also transversely cut to clean off the fascia. Each muscle graft was then used to create an RPNI in the recipient rat by neurotizing it with the residual end of the transected common peroneal nerve (see the Surgical Procedure section). For the negative control group (Group 5), the left common peroneal nerve underwent transection without RPNI construction. After 3 mo of convalescence to permit axonal regeneration and muscle reinnervation, all RPNIs underwent in situ needle EMG recordings in response to electrical stimulation of the proximal common peroneal nerve, followed by muscle force testing. All RPNIs and nerves were subsequently harvested for histological assessment.

2.3 | Surgical procedure

Animals were anesthetized in an induction chamber using a solution of 5% isoflurane in oxygen at 0.8 L/min. Anesthesia was maintained through a rebreathing nose cone, with isoflurane maintained at 2%. Analgesia was administered by subcutaneous injection of a saline dilution of 1.5 mg Rimadyl (50 mg/mL, Zoetis Inc. Parsippany, NJ). Body temperature was monitored with a skin surface probe and maintained using a heating pad. Eye lubricant was applied for corneal protection and a 5-mL subcutaneous injection of 0.9% saline was provided for hydration. In four experimental groups, a single RPNI per animal was created using a donor SM muscle graft with weights detailed in the Experimental Design section. In RPNI rats, an incision was made on the lateral aspect of the left thigh and dissection proceeded deep to the biceps femoris until the sciatic nerve was exposed. The peroneal nerve was carefully dissected and cut proximal at its entrance into the lateral compartment of the lower leg. Each free muscle graft from donor rats was then transferred to the lateral left thigh of the anesthetized recipient RPNI rat. The muscle graft was anchored proximally to the periosteum of the femur, lay along the coronal plane between the deep vastus lateralis and the biceps femoris muscles and was attached near the cartilage of the knee using 6-0 Prolene® suture (Ethicon, New Brunswick, NJ). To achieve neurotization, a small centrally located superficial incision was made in the muscle graft; the residual end of the transected common peroneal nerve was implanted into the incision and secured with 10-0 nylon suture (Ethicon, New Brunswick, NJ). In all experimental animals, the left leg incision was closed in two-layers using 6-0 Vicryl® (Ethicon, New Brunswick, NJ) for the superficial muscular layer and 5-0 chromic gut suture (Ethicon, New Brunswick, NJ) for the skin. All surgical procedures were performed by the same surgeon.

2.4 | Endpoint evaluations

2.4.1 | EMG

Nerve conduction studies were performed at 3 mo postoperatively to determine reinnervation of the RPNI and the capacity of RPNIs to

transduce nerve signals.[13] Each rat was anesthetized as described above, with body heat maintained at 35°C. The surgical site was re-opened to expose the surface of the RPNI. The common peroneal nerve was subsequently isolated proximally with care taken to avoid injury to the nerve. In situ bipolar needle EMG was then performed using stainless steel needle recording electrodes, (112-812-48TP, Grass Technologies, Warwick, Rhode Island, USA) placed in the center of the RPNI, and a reference electrode of similar type placed just proximal to the distal anchor site of the RPNI. The ground needle electrode was placed in the contralateral first toe web space. A bipolar stainless steel hook electrode (501650, Harvard Apparatus, Holliston, Massachusetts, USA) was placed on the common peroneal nerve approximately 5 to 8 mm proximal to the entry point of the nerve into the RPNI and was used to deliver electrical stimuli. Stimulation pulses were generated and evoked EMG signals recorded using a TECA Synergy T2X Clinical Nerve Conduction Study System (Viasys Healthcare, Madison, WI). Biphasic stimulation pulses were varied from 0 to 15 mA in 0.03 mA increments at a repetition rate of 1.0 Hz and phase duration of 0.1 ms. The stimulation amplitude was increased until a compound muscle action potential (CMAP) was recorded as well as a point 20% past the CMAP stimulation threshold, to ensure maximal muscle contractility (Supporting Information Figure S1A, which is available online).

2.4.2 | Muscle force testing

The health and function of the RPNI was assessed in situ via the maximum tetanic isometric force (F_0) in response to electrical stimuli delivered to the nerve using a previously described protocol.[23-25] Briefly, the anesthetized rat was placed on a platform and the femoral condyle and foot were firmly secured. The proximal tendon of the SM muscle was dissected free from the femoral periosteum. A suture loop secured to the freed tendon was used to attach the muscle graft to a servomotor calibrated force transducer (Model 300H, Cambridge Technology Inc., Cambridge, MA) connected to a LabVIEW data acquisition system (National Instruments, Austin, TX). A bipolar hook electrode was placed on the nerve (see the EMG section) and used to deliver supramaximal stimuli (square pulses, 0.2-ms pulse duration, 2-6 V) generated by a voltage stimulator (Model S88, Grass Instrument Co., Quincy, MA). Twitch contractions in response to these electrical stimuli were used to determine the optimal muscle length (L_0) for force production. Maximum isometric tetanic force (F_0) was assessed by stimulating the muscle graft as above for 250 ms at increasing frequencies from 30 to 220 Hz, up to six times, or until a force plateau was reached. A rest interval of 2 min between each tetanic contraction was employed to permit muscle recovery (Supporting Information Figure S1B). During testing, the RPNI was regularly bathed with warm mineral oil (36°C), and body temperature was monitored and maintained between 35 and 36°C.
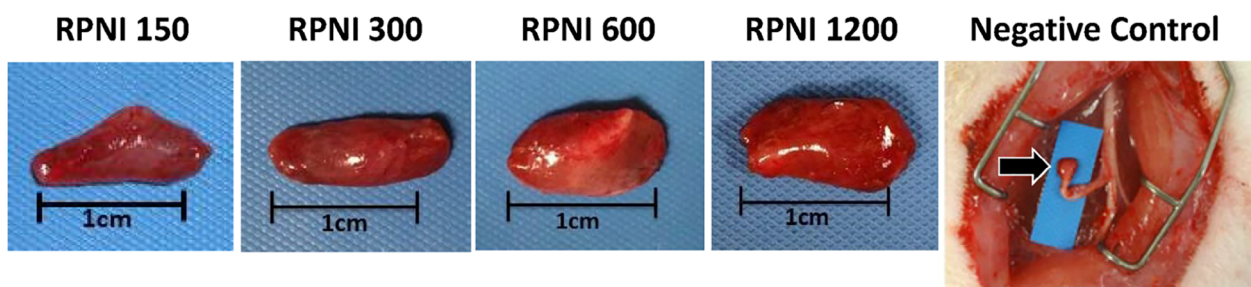
FIGURE 1 RPNI constructs at study endpoint. The RPNI 150, 300, 600, 1200, and negative control images are representative of the gross muscle observed at 3 mo. Upon inspection, RPNIs revealed innervated healthy vascularized muscle grafts, while all negative controls developed neuromas of various sizes at the ends of the transected nerves (denoted by black arrow) [Color figure can be viewed at wileyonlinelibrary.com]

TABLE 1 Summary of RPNI muscle graft characteristics at time of surgery and at endpoint testing after 3 months

Study variables	RPNI 150	RPNI 300	RPNI 600	RPNI 1200
Implant muscle mass (mg)	171 ± 6	329 ± 7 *	614 ± 9 *†	1213 ± 18 *†‡
Final muscle mass (mg)	72 ± 7	98 ± 4	134 ± 10 *	183 ± 13 *†‡
Muscle mass retained (%)	41.7 ± 3.7	29.8 ± 1.1 *	21.9 ± 1.7 *	15.0 ± 1.1 *†‡
CSA (mm^2)	7.1 ± 0.8	9.5 ± 0.7	12.6 ± 0.9 *	13.9 ± 1.2 *†
CMAP amplitude (mV)	6.6 ± 1.3	4.7 ± 0.8	3.1 ± 0.6 *	2.3 ± 0.7 *‡
Tetanic force (mN)	289.0 ± 43.3	257.7 ± 49.1	235.0 ± 75.8	91.1 ± 25.3 *†‡
Specific force (N/mm^2)	44.9 ± 8.7	29.1 ± 6.4	17.3 ± 5.2 *	5.9 ± 1.3 *†

Note: Values are mean ± SEM. *P*-value indicates significance level for main effects one-way ANOVA. Bonferroni post-hoc comparisons:
*Significantly different compared to RPNI 150 ($P < .05$). †Significantly different compared to RPNI 300 ($P < .05$).
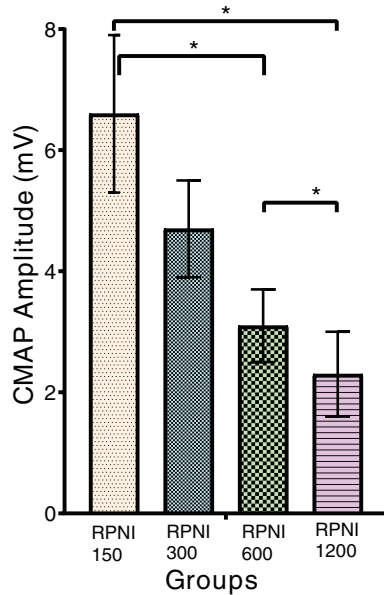‡Significantly different compared to RPNI 600 ($P < .05$).
Abbreviations: mm^2, millimeters squared; mN, millinewtons; N, Newtons.

The total muscle fiber physiologic cross-sectional area (CSA) was calculated according to the formula in Equation (1).[26]

$$CSA = \frac{SM_{MASS} \times \cos\theta}{\rho \times L_O \times 0.72} \qquad (1)$$

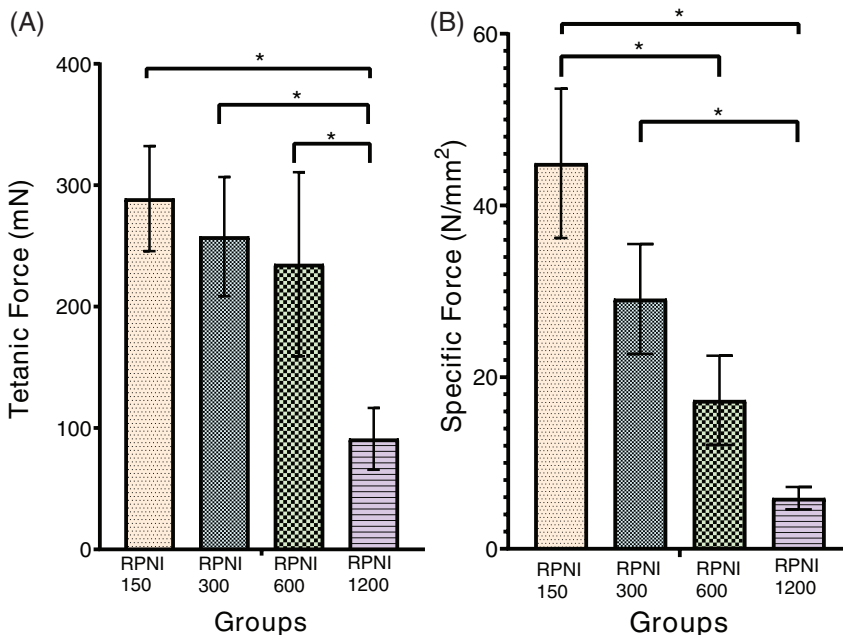where, SM_{MASS} = muscle mass at harvest (mg), θ = angle of pennation (2.1 for the rat SM muscle), ρ = density of mammalian skeletal muscle of 1.06 (kg/L), L_O = optimal muscle length for force production determined during testing (mm), and 0.72 = the ratio of muscle fiber to whole muscle length for the rat SM muscle.[27] The maximum specific isometric tetanic force (sF_O) was calculated as the F_O normalized to muscle physiologic CSA.

2.4.3 | Histology

Following endpoint testing, each RPNI was harvested and fixed in 10% formalin. Muscle tissue regeneration and reinnervation were evaluated with light microscopy. Half of the samples from each group underwent henatoxylin and eosin (H&E) staining using tissue cross-sections obtained from one-fourth and one-half the muscle lengths. The remainder were stained with Masson trichrome. The distal peroneal nerve tissue was fixed in Karnovsky's fixative (Electron Microscopy Sciences Inc., Hatfield, PA). Cross-sections of the distal nerve were stained with 1% toluidine blue for myelin. Evaluation of nerve architecture was performed under light microscopy.

2.5 | Statistical analysis

Comparisons of means for muscle mass, CMAP amplitude, tetanic force, and CSA between groups were performed with a one-way analysis of variance (ANOVA) with a Bonferroni post hoc analysis. A repeated measures ANOVA was used to calculate differences in mean muscle mass upon initial surgery and endpoint evaluations between different groups. Pearson correlation coefficients were calculated by bivariate linear regression to judge the relationship strength between: (a) initial mass and change in muscle mass, and (b) CMAP amplitude and final RPNI mass. Statistical significance was set at $P \leq .05$. All statistical analyses were performed via SPSS 25 (IBM, Armonk, NY, USA).

FIGURE 2 CMAP amplitudes as a function of RPNI muscle graft mass. RPNIs constructed with 600 and 1200 mg muscle grafts generated significantly lower CMAPs than 150 mg RPNIs. Values are represented as mean ± SEM, *P < .05 [Color figure can be viewed at wileyonlinelibrary.com]

FIGURE 3 RPNI force generation as a function of muscle graft mass. A, Maximal isometric force. B, The sF_O of RPNI constructs. Values are mean tetanic force ± SD normalized by physiological CSA, which is a function of muscle mass and length. Values are mean ± SEM. * indicates significantly lower than 150 mg RPNIs, P < .05 [Color figure can be viewed at wileyonlinelibrary.com]
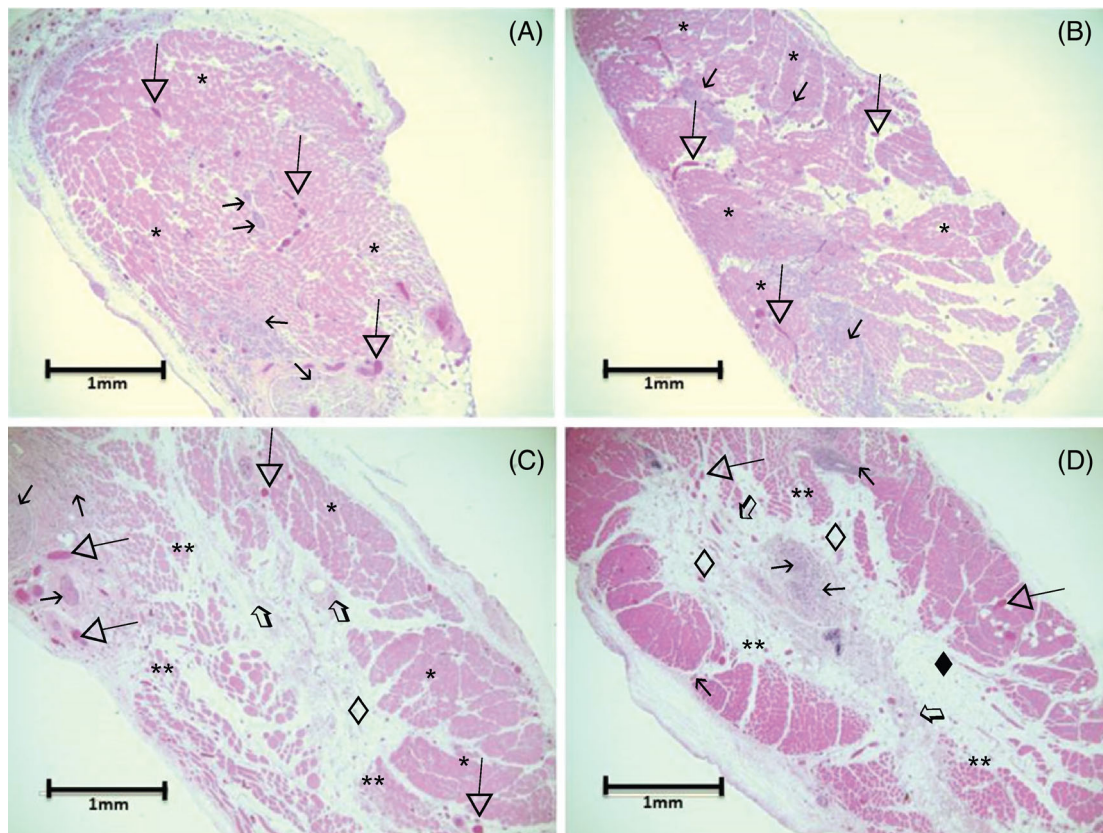
FIGURE 4 Representative cross-sections of the central part of RPNI muscle grafts stained with H&E. A, Normal muscle fiber (*), nerve (↑), and vascular (∇ [open head arrow with tail]) architecture was observed in the RPNI 150 constructs. B, RPNI 300 muscle tissue is normal. C, Central fibrosis (⇑), fat accumulation (◇), and atrophic muscle fibers (**) apparent in the RPNI 600 harvests. D, RPNI 1200 muscle grafts showed evident central fibrosis and fat deposition, with regenerated muscle fibers only at the periphery [Color figure can be viewed at wileyonlinelibrary.com]

3 | RESULTS

All rats recovered from the initial surgery without complications. On gross inspection, all RPNIs appeared healthy and displayed robust revascularization (Figure 1). The negative control group demonstrated bulbous swellings on the end of the transected nerve indicating neuroma formation.

RPNI muscle graft characteristics are summarized in Table 1. Muscle mass was significantly reduced in all experimental groups, compared to its initial graft mass, with the biggest proportional change observed in the RPNI 1200 group. The amount of muscle mass lost was significantly different between all groups (P < .001). Regression analysis demonstrated a strong correlation (r = 0.9) between initial muscle mass at the time of RPNI surgery and muscle mass recorded 3 mo postoperatively.

3.1 | EMG

All RPNIs exhibited visible muscle graft contractions and robust EMG signals upon electrical stimulation of the common peroneal nerve. Maximum CMAP amplitudes were statistically different between groups, with RPNI 150 and RPNI 300 cohorts demonstrating mean and SEM of 6.6 ± 1.3 mV and 4.7 ± 0.9 mV, respectively (Figure 2). Significantly lower

CMAPs were observed in the RPNI 600 (3.1 ± 0.6 mV) and RPNI 1200 (2.3 ± 0.7 mV) groups compared to the RPNI 150 group. Regression analysis indicated there is a significant declining trend in the maximum CMAP amplitudes generated by larger RPNI muscle grafts (r = −0.7).

3.2 | Muscle force

All RPNIs were capable of generating muscle force contractions in response to an evoked neural stimulus, indicating robust reinnervation. The F_0 generated by RPNI 150, 300, and 600 cohorts were statistically similar, with means and SEMs of 289.0 ± 43.3, 257.7 ± 49.1, and 198.8 ± 71.7 mN, respectively (Figure 3A). Tetanic forces recorded from the RPNI 1200 group (116.4 ± 31.0 mN) were significantly lower in comparison to the others. When physiological CSA was used to calculate sF_0, the RPNI 600 and 1200 groups were significantly lower than RPNI 150 and 300 cohorts (Figure 3B).

3.3 | Histology

In the RPNI 150 and RPNI 300 groups, light microscopy examination of H&E stained muscles revealed healthy organized muscle tissue
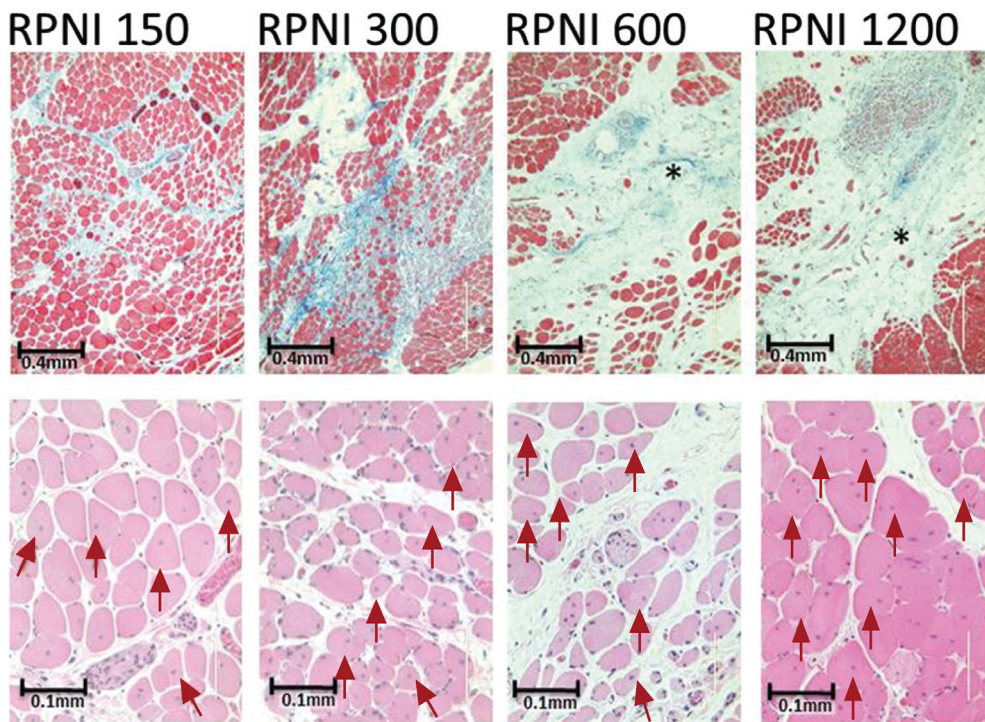
FIGURE 5 Representative high power images of RPNI muscle graft histology. Top: Masson's Trichrome stained cross-sections of RPNI muscles, central part. Note the gradual increase in central atrophy and resorption area (*). Bottom: H&E stained cross-sections of RPNI muscles. Smaller RPNI 150 mg and RPNI 300 mg muscle grafts showed healthy regenerated fibers as demonstrated by centrally nucleated myofibers (arrows) and a normal architecture with little intramuscular connective tissue. Note the swollen myofibers in the RPNI 1200 muscle [Color figure can be viewed at wileyonlinelibrary.com]
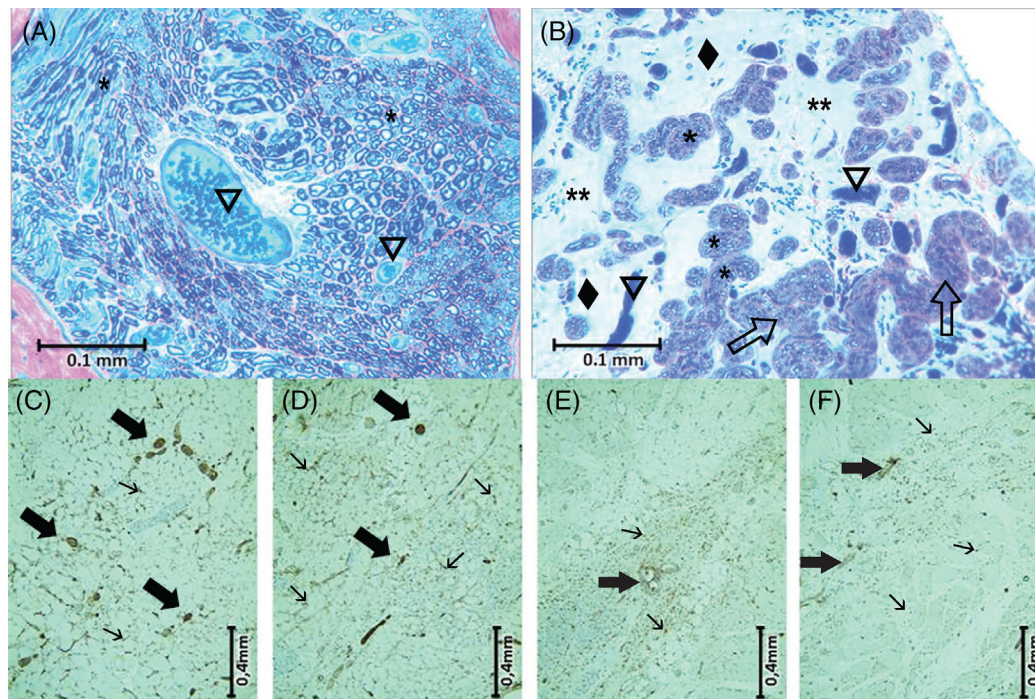
FIGURE 6 A, Innervating peroneal nerve of RPNI 300 construct. Myelinated axons (*), blood vessels (▽). Multidirectional axonal sprouting occurs into the muscle graft. B, Part of the bulbous swelling (◆) of a neuroma excised from the transected nerve of a negative control rat. Note the increased space between nerve fibers (**) and the lack of organized fibrils (⇑). C-F, Cross-sections of RPNIs stained for vwf. The 150 (C) and 300 (D) RPNIs show increased vascularization compared to the 600 (E) and 1200 (F) RPNI groups. Arrows indicate positive VWF blood vessels (large arrow) and capillaries (↑) [Color figure can be viewed at wileyonlinelibrary.com]

architecture with little fibrosis (Figure 4A,B). However, both the RPNI 600 and RPNI 1200 constructs showed either limited or no regeneration in the central area of the muscle tissue, respectively. Fibrosis and fat deposition became more evident within these larger RPNIs (Figure 4C,D). Myofibers displayed various stages of maturation, with a relative increase in the ratio of immature muscle fibers with centrally

located nuclei and large mature fibers with a peripheral nucleus in muscle grafts of all groups (Figure 5). In contrast to both the 150 and 300 RPNI groups, histomorphometrical analysis demonstrated that there was a consistent finding of disorganized axonal sprouting and evidence of neuroma formation (Figure 6A,B). Capillary density was assessed using von Willebrand factor (vwf) histology. Upon examination of cross-sections of RPNIs, positive staining for vwf was seen in both the 150 and 300 RPNI groups (Figure 6C,D); however, this was not observed for either the 600 or 1200 RPNI group (Figure 6E,F).

4 | DISCUSSION

While larger RPNIs were found to be capable of signal transduction and myocontractile force generation, the results of the present study demonstrate that both CMAP amplitude and muscle force are significantly decreased when a muscle mass higher than 300 mg is implanted in the rat model. Our results suggest that the optimal RPNI muscle mass is between 150 to 300 mg in this rat model, when the common peroneal nerve is used to reinnervate the RPNI.

Electrical signal performance of all RPNIs was assessed using CMAP amplitude in response to an electrical stimulus applied proximally to the peroneal nerve. All RPNIs yielded easily detectable CMAPs, but 1200 mg RPNIs saw a significant decrease in CMAP output. This decrease may be explained by the lack of viable muscle fibers in the central area of the muscle tissue, with increasing amounts of fibrosis throughout the remainder of the RPNI 1200 constructs. The non-functional tissue observed in the central aspect of the larger RPNIs cannot be reinnervated and as a result, does not contribute to signal transduction. The slightly smaller CMAPs generated by the RPNI 300 constructs in comparison to the RPNI 150 group can be attributed to the increased amounts of immature centrally nucleated myofibers observed in the former.

These smaller, immature fibers, while capable of signal transduction, contribute less to the contractility of the overall muscle, and by extension, to a lower summation of action potentials forming the basis of the CMAP.[28] Nevertheless, it is noteworthy that all recorded CMAPs were in the millivolt range, resulting in signals that are at least 80 times greater than similar recordings performed with electrodes placed directly on peripheral nerves.[6] In this situation, central necrosis by itself is not a limiting factor since both the 600 and 1200 RPNI group achieved signal averages of 3 and 2.3 mV, respectively. Therefore, the increased SNR available for prosthetic control as a result of signal amplification in the RPNIs are advantages inherent to even large RPNIs.[29] However, it is also easy to see that if the muscle graft used for creation of the RPNI is too large, it may adversely impact the efferent motor action potential amplification.

Maximum tetanic isometric forces were recorded to evaluate overall muscle health and functional recovery after RPNI construction. As the muscle mass used to construct the RPNI was increased, the muscle force generation decreased. When muscle force is normalized to the physiologic muscle CSA, the sF_0 decreases even more dramatically, and significantly so in the RPNI 600 and RPNI 1200 constructs,

indicating more non-contractile elements in these RPNIs, which add to the graft mass, but do not contribute to force generation. The histological observations of harvested RPNIs verify these conclusions, as we observed higher numbers of immature muscle fibers, and increases in fibrosis centrally in larger RPNIs. This leads to lower myofiber contractile forces, and fewer fibers per muscle area contributing to force generation, respectively. This finding is most evident with the declining sF_0 in the RPNIs created with larger muscle grafts.

The histological assessments performed in this study help explain RPNI function, but also that of nerve regeneration in the presence or absence of denervated target tissue. The lack of any identified neuroma formation in any of the RPNI groups demonstrates sufficient muscle reinnervation to prevent ongoing pathologic axonal sprouting and elongation resulting in a neuroma. This is further exemplified by the lack of neuromas seen in the larger RPNI groups that displayed central necrosis. We can postulate two potential mechanisms for this phenomenon: (a) all of the axons seeking reinnervation were provided an appropriate muscle fiber for reinnervation, even in the 1200 RPNI group with central necrosis;and/or (b) something in the milieu of the larger RPNI groups prevented neuroma formation even when there were not enough muscle fibers for every regenerating axon. In contrast to the RPNI groups, disorganized axon sprouting and qualitative histologic evidence of neuroma was found within the negative control group. This observation confirms our understanding that ongoing nerve regeneration will form a neuroma when there is no denervated target muscle available for reinnervation. Experimental and clinical trials support this observation in both the rodent and human population.[30-32]

Overall, this investigation of RPNI viability and performance as a function of muscle graft size supports the contention that free skeletal muscle grafting is most successful with smaller muscle grafts (<500 mg) in the rat model. As previously noted by Carlson and Guttman, the ischemic muscle fibers of the central zone in a small muscle graft are replaced by regenerated muscle fibers, while in larger grafts, the original muscle fibers of the central zone are replaced by a core of dense fibrous connective tissue.[31,33] Our results align with Carlson's hypothesis that the upper limit in rats is a muscle graft of 500-1000 mg.

For application of muscle regeneration techniques to humans, dimensionality is very important, especially in free muscle grafting models like the RPNI. Free grafting is size limited and there is some species variation in the response of muscle to free grafting. In rats, research by Woo et al. used five different muscle types for creation of RPNIs: whole EDL, partial biceps femoris, partial rectus femoris, partial lateral gastrocnemius, and partial vastus medialis.[34] Each graft was approximately 140 mg and neurotized by the common peroneal nerve. After 4 mo, in situ EMG and force testing demonstrated detectable EMG signals, suggesting that a variety of partial and whole muscles can be used to create functional RPNIs.[34] Free skeletal muscle grafting has also been successful in cats.[35,36] However, RPNIs performed in non-human primates (NHPs) differed slightly in that the center of a free graft develops a core of collagenous connective tissue, surrounded by a concentric rim of regenerated muscle fibers.[37]

Despite lacking a functional center, RPNIs in NHPs have demonstrated volitional amplified signal transduction in vivo capable of controlling a prosthetic hand,[20] supporting the argument that the measure of success in free grafting models is a function of the completeness of axonal reinnervation and not muscle regeneration.[38]

We acknowledge certain limitations of the current study. Our model is the rat, and we cannot say for absolute certain if these results would directly translate to a larger animal model with larger nerves. Peripheral nerves have their own vascular supply, and as such, can contribute to revascularization of the muscle when they are larger. This could potentially mean that larger muscle grafts may work better in humans. Second, strategically placing RPNIs in a better vascularized bed may provide revascularization and more viable muscle for larger signals. Our lab is currently assessing this. Last, only one muscle was tested in our rodent model. It is possible, therefore, that the results could be different with muscles that have different architecture from one another.

In summary, the presence of neuroma was not seen in any of the RPNI groups. RPNI electrical signaling is optimal in the rat model when smaller masses of free skeletal muscle grafts (150-300 mg) are used. Larger masses of free skeletal muscle grafts (600-1200 mg) are capable of amplifying efferent motor action potentials; however, due to a larger amount of denervated muscle fibers and central necrosis, the CMAP amplitudes are diminished. These results are critical to our understanding the ability of RPNIs to amplify efferent motor action potentials for control of prosthetic devices.

ACKNOWLEDGEMENTS

CONFLICT OF INTEREST

None of the authors has any conflict of interest to disclose.

ETHICAL PUBLICATION STATEMENT

We confirm that we have read the Journal's position on issues involved in ethical publication and affirm that this report is consistent with those guidelines.

ORCID

Stephen W. P. Kemp https://orcid.org/0000-0002-5608-3584

REFERENCES

1. Miranda RA, Casebeer WD, Hein AM, et al. DARPA-funded efforts in the development of novel brain-computer interface technologies. *J Neurosci Methods*. 2015;244:52-67.
2. Ryait HS, Arora AS, Agarwal R. Study of issues in the development of surface EMG controlled human hand. *J Mater Sci Mater Med*. 2009;20 (Suppl 1):S107-S114.
3. Engdahl SM, Christie BP, Kelly B, Davis A, Chestek CA, Gates DH. Surveying the interest of individuals with upper limb loss in novel prosthetic control techniques. *J Neuroeng Rehabil*. 2015;12:53.
4. Biddiss EA, Chau TT. Upper limb prosthesis use and abandonment: a survey of the last 25 years. *Prosthet Orthot Int*. 2007;31(3):236-257.
5. Ursu DC, Urbanchek MG, Nedic A, Cederna PS, Gillespie RB. In vivo characterization of regenerative peripheral nerve interface function. *J Neural Eng*. 2016;13(2):026012.
6. Navarro X, Krueger TB, Lago N, Micera S, Stieglitz T, Dario P. A critical review of interfaces with the peripheral nervous system for the control of neuroprostheses and hybrid bionic systems. *J Peripher Nerv Syst*. 2005;10(3):229-258.
7. Thil MA, Duy DT, Colin IM, Delbeke J. Time course of tissue remodelling and electrophysiology in the rat sciatic nerve after spiral cuff electrode implantation. *J Neuroimmunol*. 2007;185(1–2):103-114.
8. Tan DW, Schiefer MA, Keith MW, Anderson JR, Tyler J, Tyler DJ. A neural interface provides long-term stable natural touch perception. *Sci Transl Med*. 2014;6(257):257ra138.
9. Thota AK, Kuntaegowdanahalli S, Starosciak AK, et al. A system and method to interface with multiple groups of axons in several fascicles of peripheral nerves. *J Neurosci Methods*. 2015;244:78-84.
10. Jia X, Koenig MA, Zhang X, Zhang J, Chen T, Chen Z. Residual motor signal in long-term human severed peripheral nerves and feasibility of neural signal-controlled artificial limb. *J Hand Surg Am*. 2007;32(5): 657-666.
11. Hargrove L, Zhou P, Englehart K, Kuiken TA. The effect of ECG interference on pattern-recognition-based myoelectric control for targeted muscle reinnervated patients. *IEEE Trans Biomed Eng*. 2009; 56(9):2197-2201.
12. Jiang N, Englehart KB, Parker PA. Extracting simultaneous and proportional neural control information for multiple-DOF prostheses from the surface electromyographic signal. *IEEE Trans Biomed Eng*. 2009;56(4):1070-1080.
13. Kung TA, Langhals NB, Martin DC, Johnson PJ, Cederna PS, Urbanchek MG. Regenerative peripheral nerve interface viability and signal transduction with an implanted electrode. *Plast Reconstr Surg*. 2014;133(6):1380-1394.
14. Ursu D, Nedic A, Urbanchek M, Cederna P, Gillespie RB. Adjacent regenerative peripheral nerve interfaces produce phase-antagonist signals during voluntary walking in rats. *J Neuroeng Rehabil*. 2017;14 (1):33.
15. Frost CM, Ursu DC, Flattery SM, et al. Regenerative peripheral nerve interfaces for real-time, proportional control of a Neuroprosthetic hand. *J Neuroeng Rehabil*. 2018;15(1):108.
16. Vu PP, Irwin ZT, Vaskov AK, et al. A regenerative peripheral nerve interface allows real-time control of an artifical hand in upper limb amputees. *Sci Transl Med*. 2020;12(533):1–11.
17. Svientek SR, Ursu DC, Cederna PS, Kemp SWP. Fabrication of the composite regenerative peripheral nerve interface (C-RPNI) in the adult rat. *JoVE*. 2020;156:1–14.
18. Kubiak CA, Kemp SWP, Cederna PS. Regenerative peripheral nerve Interface for Management of Postamputation Neuroma. *JAMA Surg*. 2018;153(7):681-682.
19. Kubiak CA, Kemp SWP, Cederna PS, Kung TA. Prophylactic regenerative peripheral nerve interfaces to prevent Postamputation pain. *Plast Reconstr Surg*. 2019;144(3):421e-430e.
20. Irwin ZT, Schroeder KE, Vu PP, et al. Chronic recording of hand prosthesis control signals via a regenerative peripheral nerve interface in a rhesus macaque. *J Neural Eng*. 2016;13(4):046007.
21. Vu PP, Irwin ZT, Bullard AJ, et al. Closed-loop continuous hand control via chronic recording of regenerative peripheral nerve interfaces. *IEEE Trans Neural Syst Rehabil Eng*. 2018;26(2):515-526.
22. Ohnishi K, Weir RF, Kuiken TA. Neural machine interfaces for controlling multifunctional powered upper-limb prostheses. *Expert Rev Med Devices*. 2007;4(1):43-53.
23. Yoshimura K, Asato H, Cederna PS, Urbanchek MG, Kuzon WM. The effect of reinnervation on force production and power output in skeletal muscle. *J Surg Res*. 1999;81(2):201-208.
24. Cederna PS, Youssef MK, Asato H, Urbanchek MG, Kuzon WM Jr. Skeletal muscle reinnervation by reduced axonal numbers results in

whole muscle force deficits. *Plast Reconstr Surg*. 2000;105(6):2003-2009.

25. Cederna PS, Asato H, Gu X, et al. Motor unit properties of nerve-intact extensor digitorum longus muscle grafts in young and old rats. *J Gerontol A Biol Sci Med Sci*. 2001;56(6):B254-B258.

26. Gans C. Fiber architecture and muscle function. *Exerc Sport Sci Rev*. 1982;10:160-207.

27. Eng CM, Smallwood LH, Rainiero MP, Lahey M, Ward SR, Lieber RL. Scaling of muscle architecture and fiber types in the rat hindlimb. *J Exp Biol*. 2008;211(Pt 14):2336-2345.

28. de Rezende Pinto WB, de Souza PV, Oliveira AS. Normal muscle structure, growth, development, and regeneration. *Curr Rev Musculoskelet Med*. 2015;8(2):176-181.

29. Ciancio AL, Cordella F, Barone R, et al. Control of prosthetic hands via the peripheral nervous system. *Front Neurosci*. 2016;10:116.

30. Ives GC, Kung TA, Nghiem BT, et al. Current state of the surgical treatment of terminal neuromas. *Neurosurgery*. 2018;83(3):354-364.

31. Carlson BM, Gutmann E. Regeneration in grafts of normal and denervated rat muscles. Contractile properties. Pflugers Arch. 1975;353(3):215-225.

32. Kung TA, Cederna PS, van der Meulen JH, Urbanchek MG, Kuzon WM Jr, Faulkner JA. Motor unit changes seen with skeletal muscle sarcopenia in oldest old rats. *J Gerontol A Biol Sci Med Sci*. 2014;69(6):657-665.

33. Carlson BM, Gutmann E. Regneration in free grafts of normal and denervated muscles in the rat: morphology and histochemistry. *Anat Rec*. 1975;183(1):47-62.

34. Woo SL, Urbanchek MG, Cederna PS, Langhals NB. Revisiting non-vascularized partial muscle grafts: a novel use for prosthetic control. *Plast Reconstr Surg*. 2014;134(2):344e-346e.

35. Maxwell LC, Faulkner JA, Mufti SA, Turowski AM. Free autografting of entire limb muscles in the cat: histochemistry and biochemistry. *J Appl Physiol Respir Environ Exerc Physiol*. 1978;44(3):431-437.

36. Tabary JC, Tabary C, Tardieu C, Tardieu G, Goldspink G. Physiological and structural changes in the cat's soleus muscle due to immobilization at different lengths by plaster casts. *J Physiol*. 1972;224(1):231-244.

37. Markley JM, Faulkner JA, Carlson BM. Regeneration of skeletal muscle after grafting in monkeys. *Plast Reconstr Surg*. 1978;62(3):415-422.

38. Carlson BM. Denervation, reinnervation, and regeneration of skeletal muscle. *Otolaryngol Head Neck Surg*. 1981;89(2):192-196.

SUPPORTING INFORMATION

Additional supporting information may be found online in the Supporting Information section at the end of this article.